ISSN 0869-5911, Petrology, 2018, Vol. 26, No. 6, pp. 640–649. © Pleiades Publishing, Ltd., 2018.
Original Russian Text © I.P. Solovova, A.A. Averin, L.O. Magazina, 2018, published in Petrologiya, 2018, Vol. 26, No. 6, pp. 659–670.

Reduced Fluids and Sulfide–Metal Alloy in the Magnesian Basalts of Disko Island, West Greenland

I. P. Solovova[a, *], A. A. Averin[a, b], and L. O. Magazina[a]

[a] *Institute of Geology of Ore Deposits, Petrography, Mineralogy, and Geochemistry, Russian Academy of Sciences, Moscow, 119017 Russia*

[b] *Frumkin Institute of Physical Chemistry and Electrochemistry, Russian Academy of Sciences, Moscow, 119991 Russia*

**e-mail: solovova@igem.ru*

Received April 6, 2018; in final form, May 28, 2018

Abstract—This paper presents the results of a combined study of the composition and physical properties of fluid, melt and opaque mineral inclusions in olivine phenocrysts and glass from the magnesian basalt of Disko I., West Greenland. The rock is dominated by glass, which contains numerous fluid bubbles and large (up to 250 μm) opaque globules. The thermometric investigation of the melt inclusions showed that the temperature of olivine crystallization was no higher than 1220°C at a pressure of 0.15–0.20 GPa. The opaque globules in the groundmass glass have a eutectoid structure and are composed of troilite, Fe–Ni metal alloy, and sparse grains of wüstite and cohenite (Fe_3C). Cryometric measurements and Raman spectroscopy indicated a complex fluid composition and presence of reduced and oxidized gases: CH_4, N_2, H_2, CO_2, and H_2O, as well as highly ordered graphite. The nonequilibrium association of compounds in the fluid is related to the rapid cooling (quenching) of crystallizing magma preventing the equilibration of the gas system. At an estimated $\log fO_2$ value of –13.95, methane is the only hydrocarbon phase that can exist at magmatic temperatures. The formation of organic substances detected in some gas bubbles in the groundmass glasses of the rock occurred at postmagmatic stages after a significant decrease in temperature.

Keywords: magnesian basalt, sulfide globule, metal alloy, fluid, inclusion, Disko Island

DOI: 10.1134/S0869591118060073

INTRODUCTION

Small drop-shaped sulfide segregations are widespread in basic rocks. Their appearance is usually attributed to silicate–sulfide liquid immiscibility during magma crystallization under subliquidus conditions. Such sulfide droplets are composed of Fe–Ni sulfides and a small amount of magnetite. Globules from lunar basalts (Blau and Goldstein, 1975) and meteorites are free of magnetite, and sulfide coexists in them with cohenite, Fe_3C, and schreibersite, $(Fe, Ni, Co)_3P$, occurring as inclusions in troilite. Less frequently, intergrowths of sulfides with Fe–Ni alloys were reported. In terrestrial rocks, metal-bearing sulfide aggregates were described in basalts from the Rhein Graben in Germany (Medenbach and ElGoresy, 1982), Siberian plateau basalts (Howarth et al., 2017), and volcanics of Disko I. and the Nûgssuaq Peninsula in West Greenland (Pedersen, 1979). The crystallization of metallic iron in equilibrium with sulfides and silicate melt requires a strongly reducing environment and an oxygen fugacity at or below the iron–wüstite buffer. Such conditions are not characteristic of basic magmas, which crystallize at oxygen fugacities close to the quartz–fayalite–magnetite buffer. Oxygen fugacity could be decreased as a result of basic magma interaction with carbonaceous crustal materials, for instance, black shales (Howarth et al., 2017). Reduced fluids must play an important role in these processes. A number of petrological investigations of natural and experimental systems with volatile components and fluid inclusion data indicate that CO_2 dominates during the crystallization of ultrabasic and basic magmas (Ryabchikov et al., 2009). However, the increasing use of Raman spectroscopy during recent decades has revealed the presence of other volatile components in fluid phases, including H_2, N_2, H_2O, H_2S, etc. (Frezzotti and Peccerillo, 2007; Dubessy et al., 1989; Solovova et al., 2015).

We investigated magnesian basalts from Disko I. and the Nûgssuaq Peninsula (West Greenland) containing sulfide globules with Fe metallic alloy. Our study focused on obtaining combined data on fluid in olivine and groundmass glass, which confirmed the low oxygen fugacity during the formation of the rock.

PETROGRAPHIC OVERVIEW

The Tertiary volcanic province of West Greenland is characterized by the abundance of picritic volcanics

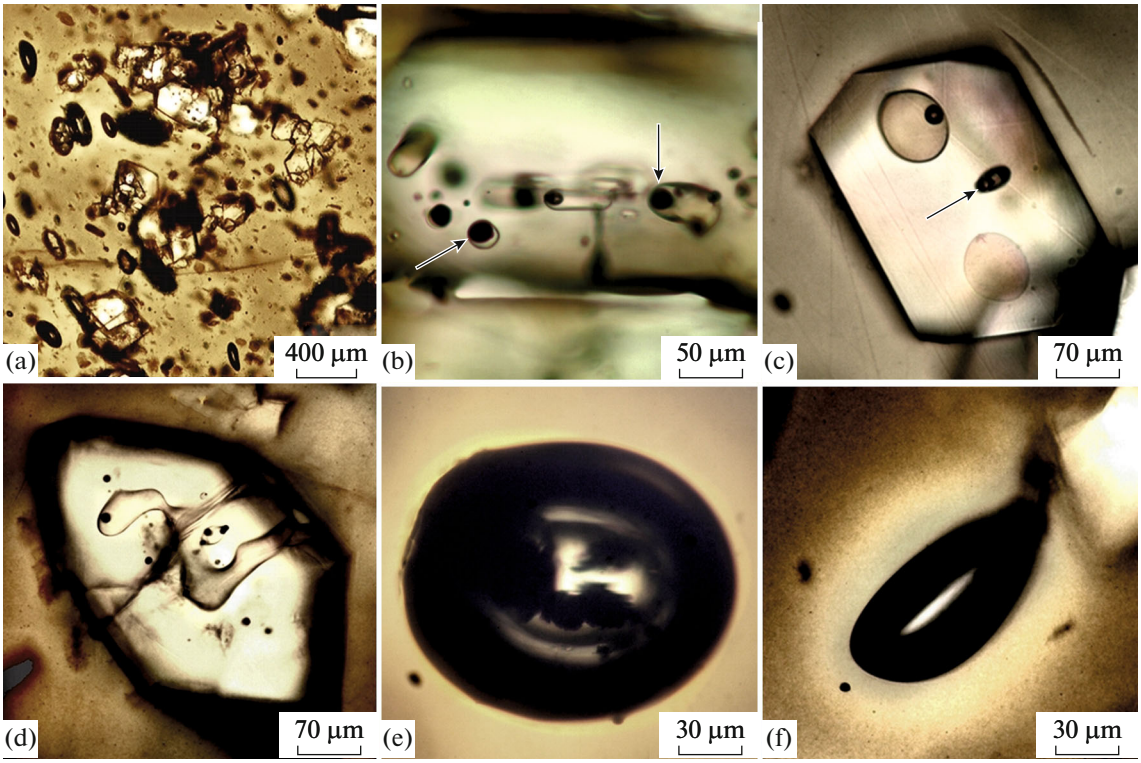

Fig. 1. Photomicrographs of basalt. (a) Olivine phenocrysts and gas bubbles in groundmass glass, general view. (b)–(d) Olivine phenocrysts with melt and fluid inclusions: (b) unheated combined graphite–melt inclusions at 20°C are indicated by arrows, (c) euhedral olivine crystal with melt and fluid (indicated by arrow) inclusions after an experiment at 1170°C, and (d) melt embayment in an olivine crystal. (e)–(f) Fluid inclusions in groundmass glass: (e) the opaque phase in the center of the inclusion is graphite, and (f) lightening of groundmass glass around a fluid bubble.

and magnesian basalts. Its geology was described in detail by Pedersen (1979). Precambrian gneisses and Early Tertiary tholeiitic basalts are cut by dikes. This fact was used as an argument for the lower crustal or upper mantle source of metallic iron (Bird and Weathers, 1977). However, this suggestion was not supported by subsequent studies. The magnesian basalts of the Vaigat Formation of Disko I. were studied by us.

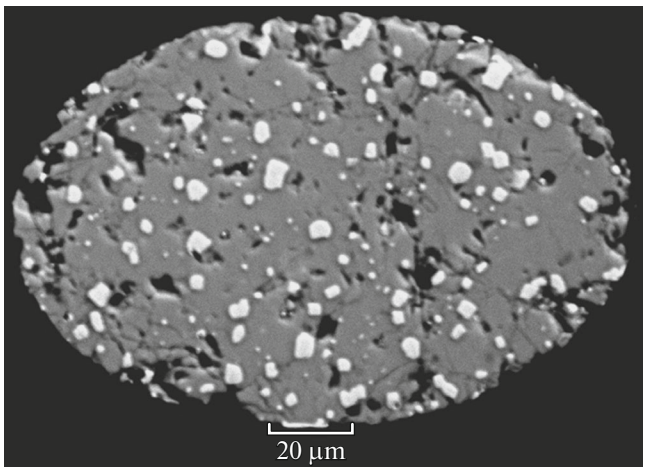

Fig. 2. Back-scattered electron image of an opaque globule in groundmass glass. Gray is sulfide, and white is Fe–Ni metallic alloy.

The basalt contains olivine phenocrysts no more than 300 μm in size. Their compositions correspond to a forsterite mole fraction of 78.8–85% ($Fo_{78.8–85}$) and include 0.19–0.30 wt % CaO. Olivine crystals are often euhedral and assembled in cluster of several grains (Fig. 1a). The rock is dominated by brownish glass accounting for no less than 80 vol %. The glass contains a few dark brown spherulites consisting of fine plagioclase (An_{74})–glass intergrowths. Olivine contains melt and fluid inclusions (Figs. 1b, 1c, 1d). A characteristic feature of the groundmass glass is the presence of abundant rounded and lenticular fluid bubbles (Figs. 1e, 1f) and multiphase opaque globules (Fig. 2), which are composed of sulfide and small grains of Fe–Ni alloy.

METHODS

The thermometric investigation of mineral-hosted inclusions was carried out using doubly polished plates up to 0.3 mm thick. Fluid inclusions were examined optically and investigated on a Linkam-THMSG 600 microscopic stage cooled with liquid nitrogen

up to −180°C. The stage was calibrated using natural and synthetic standard inclusions of CO_2 and aqueous salt solutions with a known concentration. The rates of temperature changes during cryometric measurements were maintained by an electronic control system.

The composition of fluid was estimated by Raman spectroscopy using a SENTERRA Bruker spectrometer (Frumkin Institute of Physical Chemistry and Electrochemistry, Russian Academy of Sciences, Moscow). Spectra were recorded using the 532-nm line of a Nd:YAG laser at a power of 20 mW and a spectral resolution of ~3 cm^{-1}. The time of signal acquisition was ~200 s. The spectra were recorded using a 50× objective with a scattering cross-section of ~2 μm.

The compositions of phases were determined with a JEOL JXA-8100 electron microprobe at the Institute of Geology of Ore Deposits, Petrography, Mineralogy, and Geochemistry, Russian Academy of Sciences, Moscow (analyst S.E. Borisovskii). The analytical conditions were the following: an accelerating voltage of 15 or 20 kV, a beam current of 20 or 30 nA, and an electron beam diameter of 2, 5, or 10 μm. Groundmass glasses were analyzed with an electron beam defocused to a diameter of 25 μm. The following certified standards of natural minerals and glasses were used: USNM 111240/2 (basaltic glass VG-2) for Si, Al, Fe, Mg, and Ca; jadeite for Na; orthoclase for K; rhodonite for Mn; TiO_2 for Ti; $CuFeS_2$ for Cu, Fe, and S; and metallic Ni for Ni. Sulfide inclusions were also analyzed with a JSM-5610LV (Japan) scanning electron microscope equipped with a JED-2300 (Japan) energy dispersive analytical system. The analyses were obtained at a spatial resolution of up to 1 μm, an accelerating voltage of 25 kV, and a takeoff angle of 45°. The detection limit for intermediate-mass elements was ~0.1 wt %. The spatial resolution of backscattered electron images was 400 Å.

Trace elements were measured by secondary ion mass spectrometry (SIMS) on a Cameca IMS-4f ion microprobe at the Yaroslavl Branch of the Physical Technological Institute, Russian Academy of Sciences (analyst S.G. Simakin). The measurement conditions were the following (Sobolev, 1996): the primary O^- beam was focused using a field aperture to a spot of 20 μm diameter on the sample surface, the beam current was 3–7 nA, and the energy-slit width was 50 eV. The contents of elements were calculated from their isotope ratios to ^{30}Si. The analytical uncertainty was less than 7% relative for most elements; less than 17% relative for Sm, U, Th, Hf, Yb, and Er; and less than 25% relative for Ta, Dy, and Eu.

INCLUSIONS IN OLIVINE AND GROUNDMASS GLASS

Sulfide–Metal Globules

Oval-shaped or ellipsoid sulfide globules up to 250 μm in size were observed in the groundmass glass of the rock. The sulfide is represented by coarse-grained troilite with minor chalcopyrite along the margins of the globules. In addition, the globules comprise rare grains of wüstite, cohenite (Fe_3C), and V-bearing (up to 9.5 wt % V_2O_3) spinel (Pedersen, 1979). Small (<10 μm) euhedral grains of Fe alloy are dispersed over the whole volume of the sulfide globules (Fig. 2). Their Ni content is strongly variable, and 100Ni/(Ni + Fe) ranges from 15 to 28 (Table 1). The alloy contains also up to 2.7 at % Co and 1.7 at % Cu. The structural relationships of phases in sulfide bodies indicate a uniform distribution of metal in the sulfide matrix, which allows their consideration as a eutectic assemblage (Albright and Kraft, 1966). The eutectic temperature of the binary Fe–FeS system is 988°C (Kullerud and Clark, 1959). The presence of additional components depresses this temperature. The bulk composition of the sulfide globules approaches that of the ternary Fe–Ni–S eutectic, the temperature of which is 900°C (Kullerud, 1963).

Melt Inclusions in Olivine

The melt inclusions in olivine are from 10 to 70 μm in size and were quenched under natural conditions to glass with a gas vesicle. Several gas vesicles may occur in a single inclusion; many of them are weakly transparent and are aligned perpendicular to the growth faces of the host olivine (Figs. 1b, 1c). Solid phases can be observed in the gas vesicles. The melt/fluid ratio in the inclusions is widely variable, which indicates that the magma was heterogeneous during olivine crystallization. A characteristic feature of the olivine phenocrysts is the presence of melt-filled embayments and pockets (Fig. 1d), which might be closed during late crystallization stages. This phenomenon is rare and indicates very rapid magma cooling.

The inclusions were homogenized during heating experiments at 1170–1220°C. In some experiments, the linear dimensions of inclusions were measured before and after heating to check for superheating and detect the possible presence of daughter olivine on the inclusion walls. The appearance of negative crystal faces in the host olivine was used as a criterion for the attainment of the temperature of inclusion entrapment by the growing olivine crystal. According to the measurements, daughter olivine crystals on the inclusion walls could account for no more than 15% of the inclusion volume. Note that many olivine phenocrysts were rapidly dissolved in melt upon heating above 1200°C, which could be related to the disequilibrium of early phenocrysts with low-temperature residual melts and a change in redox conditions.

Table 1. Chemical compositions of metallic alloy grains in a sulfide globule

Element	1	2	3	4	5	6	7
Fe, wt %	79.82	66.47	68.64	80.06	80.36	80.66	73.70
Co	2.75	2.55	2.16	2.91	2.41	2.70	2.68
Ni	14.94	27.19	25.71	16.74	14.69	17.69	21.53
Cu	0.55	1.70	1.44	0.55	0.54	0.67	0.86
Total	98.06	97.91	97.95	100.26	98	101.72	98.77
Fe, at %	82.19	68.04	70.75	80.03	82.25	79.70	72.63
Co	2.68	2.47	2.11	2.76	2.34	2.53	2.50
Ni	14.63	26.47	25.21	15.91	14.31	16.63	20.18
Cu	0.50	1.53	1.31	0.48	0.49	0.58	0.74
Total	100	98.51	99.38	99.18	99.39	99.44	96.05
100 × Ni(Ni + Fe)	15.1	28.0	26.3	16.6	14.8	17.3	21.7

(1–7) grains of metallic alloy in a sulfide globule

During sample heating up to 750°C, the glass of the rocks did not stick to silica glass or corundum plates, which were used as a support; i.e., the temperature of glass softening was not reached. This observation will be used during the estimation of the physical parameters of the fluid.

The analyses of melt inclusions before and after homogenization and groundmass glasses are given in Table 2 and plotted in Fig. 3. The obtained results indicate that the rock is a magnesian basalt with up to 10 wt % MgO. The analyses of homogenized melts are almost identical to the compositions recalculated to equilibrium with the host olivine, which leads to two conclusions. First, the experimental temperature was not higher than the temperature of phenocryst crystallization, which is supported by the similarity of experimental and calculated values (1170–1220°C and 1185–1237°C, respectively). Second, the diffusion exchange of Fe and Mg between phenocrysts and daughter olivine in the inclusions was negligible, probably, owing to the rapid cooling of basaltic melt during crystallization. In contrast, the compositions of naturally quenched melt inclusions are significantly different from the recalculated compositions in all major components (Fig. 3). It was estimated that equilibration with the host olivine requires the addition to the analyzed glasses of 0.061–0.165 mole fractions of olivine components, which crystallized on the inclusion walls during cooling. The naturally quenched melts in inclusions or residual melts in the presence of daughter phases are compositionally similar to the groundmass glass of the rock.

The problem of discrepancy between the compositions of melts trapped in inclusions and crystallizing magmas has often been discussed in the literature. It is related to the depletion of the zone around a growing phenocryst in elements incorporated in the crystal (for instance, Mg and Fe in crystallizing olivine). The enrichment of melt in trace elements near a crystallizing mineral was experimentally demonstrated. However, in some cases enrichment in incompatible elements was not observed in the boundary melt layer. This was established, for instance, during the investigation of naturally quenched inclusions in olivine from chondrules of the Allende stone meteorite (Florentin et al., 2018). The favorable combination of the euhedral shape of olivine crystals showing distinct faces and apexes (Fig. 1c) and the large volume of enclosing melt allowed us to analyze the groundmass glass at distances of 10 and 100 μm from crystal faces and apexes. The following contents of components were obtained (wt %): 53.68 and 53.20 SiO_2, 1.45 and 1.45 TiO_2, 16.09 and 16.39 Al_2O_3, 9.26 and 9.23 FeO, 6.74 and 6.77 MgO, 9.93 and 9.88 CaO, 2.07 and 2.33 Na_2O, and 0.66 and 0.67 K_2O, respectively. These analyses indicate that, at least in the given case, there is no difference in the composition of the proximal and remote zones of groundmass glass.

Figure 4 shows primitive mantle-normalized contents of rare earth elements (REE) in the melts. The melts of homogenized inclusions and groundmass glass show a slight LREE enrichment (La_N/Yb_N = 3.3–3.4). A weaker LREE enrichment was obtained for homogenized melt inclusions in olivine from the picrite of an older dike on Disko I. (La_N/Yb_N = 1.8). The REE distribution patterns of the melt inclusions in the basalt discussed here are transitional between those of picrites and black shales xenoliths found in some basalts (Pedersen, 1985). Thus, the LREE enrichment detected in our sample may indicate that the magma was contaminated with crustal material.

Fluid Inclusions

A characteristic feature of the basalt is the presence of numerous low-density fluid inclusions in the

Table 2. Compositions of melt inclusions and groundmass glass, wt %

Component	1	2	3	4	5	6	7	8	9	10	11	12	13
SiO_2	54.59	53.80	49.58	50.81	50.08	52.00	48.80	49.82	49.90	50.40	53.34	49.68	53.18
TiO_2	1.58	1.47	1.84	1.56	1.55	1.44	1.59	1.89	1.65	1.60	1.44	1.59	1.51
Al_2O_3	15.90	15.31	17.64	17.11	16.92	14.81	17.35	16.59	17.01	16.36	14.71	16.92	15.60
FeO	8.56	8.44	9.75	9.36	8.88	10.59	9.81	10.10	9.17	9.87	9.65	9.84	9.18
MnO	0.14	0.26	0.11	0.13	0.15	0.22	0.07	0.20	0.18	0.20	0.11	0.16	0.14
MgO	6.51	7.15	8.35	8.44	8.46	8.54	8.69	8.71	8.84	8.92	8.95	9.04	9.15
CaO	10.06	11.07	10.24	9.52	9.44	10.78	10.82	9.93	9.99	9.54	9.41	9.65	9.14
Na_2O	1.11	1.97	1.85	2.25	2.09	1.87	2.28	1.98	2.36	2.30	1.82	2.25	1.98
K_2O	0.67	0.59	0.68	0.77	0.73	0.50	0.54	0.72	0.77	0.75	0.46	0.83	0.56
Total	99.12	100.06	100.04	99.95	98.30	100.75	99.95	99.94	99.87	99.94	99.89	99.96	100.44
*Ol**	81.1	83.3	82.2	83.7	83.7	81.3	83.4	82.2	83.7	83.7	83.2	83.0	84.0
Compositions of melt recalculated to equilibrium with host olivine assuming $Kd = 0.33$													
SiO_2	54.76	53.08	49.57	50.45	50.97	51.64	48.51	49.92	49.99	49.99	53.43	49.75	53.09
TiO_2	1.57	1.41	1.84	1.51	1.58	1.43	1.54	1.90	1.66	1.55	1.45	1.60	1.52
Al_2O_3	15.76	14.63	17.65	16.60	17.25	14.73	16.85	16.70	17.14	15.85	14.81	17.07	15.74
FeO	8.96	9.14	9.73	9.80	9.00	10.48	10.24	10.02	9.06	10.29	9.55	9.69	8.92
MnO	0.14	0.26	0.11	0.13	0.15	0.22	0.07	0.20	0.18	0.20	0.11	0.16	0.14
MgO	7.08	8.45	8.32	9.33	8.55	8.42	9.54	8.55	8.61	9.78	8.75	8.75	8.66
CaO	9.97	10.59	10.25	9.24	9.62	10.72	10.52	9.99	10.07	9.25	9.47	9.73	9.22
Na_2O	1.10	1.88	1.85	2.18	2.13	1.86	2.21	1.99	2.38	2.23	1.83	2.27	2.00
K_2O	0.66	0.56	0.68	0.75	0.74	0.50	0.52	0.72	0.78	0.73	0.46	0.84	0.57
*Ol***	0.018	0.045	−0.001	0.031	−0.002	−0.002	0.030	−0.006	−0.008	0.031	−0.007	−0.01	−0.015
T, °C	1185	1209	1206	1230	1214	1207	1228	1212	1214	1237	1216	1218	1215
#*Mg* of melt	0.58	0.62	0.60	0.63	0.63	0.59	0.62	0.60	0.63	0.63	0.62	0.62	0.63

Table 2. (Contd.)

Component	14	15	16	17	18	19	20	21	22	23	24	25
SiO_2	53.80	52.92	53.21	53.33	53.08	53.65	54.13	54.96	53.58	53.78	53.87	53.68
TiO_2	1.59	1.56	1.49	1.47	1.46	1.66	1.64	1.75	1.45	1.57	1.56	1.45
Al_2O_3	16.45	16.27	16.61	16.31	16.22	17.02	15.49	13.43	15.29	15.42	15.31	16.09
FeO	8.25	8.78	8.82	8.96	9.17	8.24	8.94	10.04	8.98	8.79	8.84	9.26
MnO	0.15	0.15	0.15	0.17	0.15	0.16	0.00	0.17	0.12	0.16	0.00	0.14
MgO	4.93	4.88	4.31	5.15	5.24	4.28	4.82	8.03	6.06	6.71	7.01	6.74
CaO	12.01	11.67	12.08	11.97	12.14	12.77	11.56	9.29	10.99	10.20	9.92	9.93
Na_2O	2.11	2.12	2.37	1.98	1.89	2.17	2.06	1.12	2.21	2.20	2.33	2.07
K_2O	0.60	0.57	0.62	0.60	0.53	0.59	0.57	0.97	0.66	0.63	0.33	0.66
Total	99.89	98.92	99.65	99.94	99.88	100.54	99.21	99.76	99.34	99.46	99.17	100.02
*Ol**	78.8	78.8	78.8	78.8	78.8	78.8						
Compositions of melt recalculated to equilibrium with host olivine assuming $Kd = 0.33$												
SiO_2	52.87	51.93	50.88	52.03	51.76	51.43						
TiO_2	1.50	1.43	1.27	1.35	1.34	1.46						
Al_2O_3	15.50	14.90	14.15	15.01	14.86	14.96						
FeO	9.53	10.91	12.25	10.68	10.98	10.85						
MnO	0.15	0.15	0.14	0.17	0.15	0.16						
MgO	6.57	7.52	8.43	7.36	7.56	7.47						
CaO	11.33	10.71	10.33	11.03	11.14	11.25						
Na_2O	1.99	1.94	2.02	1.82	1.73	1.91						
K_2O	0.56	0.52	0.53	0.55	0.49	0.52						
*Ol***	0.061	0.100	0.165	0.085	0.090	0.125						
T, °C	1173	1191	1210	1188	1190	1190						
#*Mg* of melt	0.55	0.55	0.55	0.55	0.55	0.55						

1–13, homogenized inclusions; 14–19, naturally quenched inclusions; and 20–25, groundmass glass of the rock. *Ol** is the composition of host olivine, *Ol*** is the mole fraction of added olivine, and *T*, °C is the estimated temperature of inclusion homogenization.

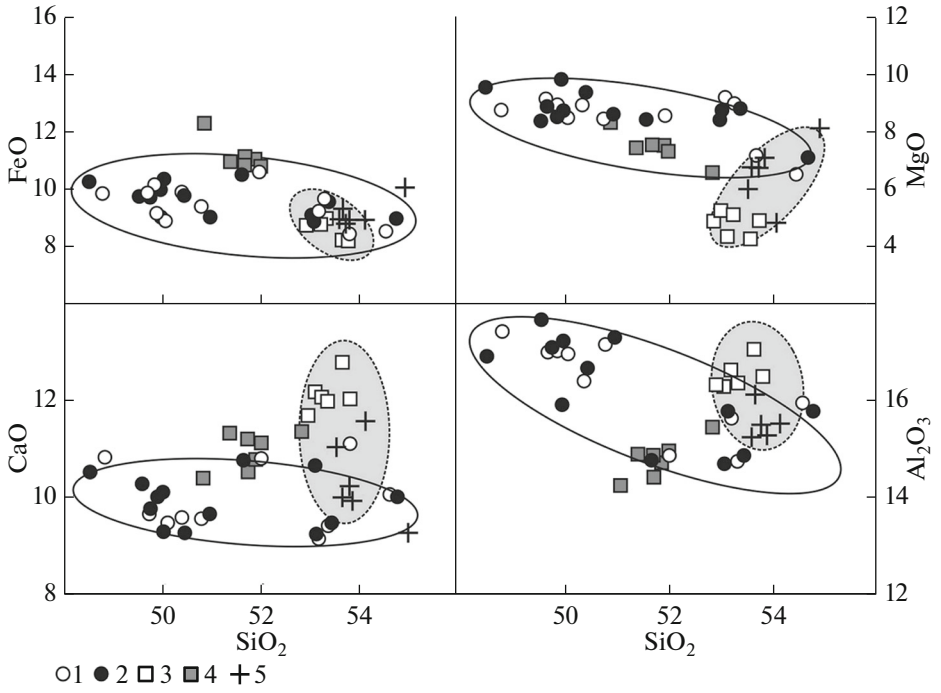

Fig. 3. Variations in the contents of major components in melts as functions of SiO_2 content, wt %. The diagram shows the compositions of (1) glasses from homogenized inclusions and (2) corresponding melts recalculated to equilibrium with the host mineral, (3) naturally quenched inclusions and (4) corresponding melts recalculated to equilibrium with the host olivine, and (5) groundmass glass of the rock.

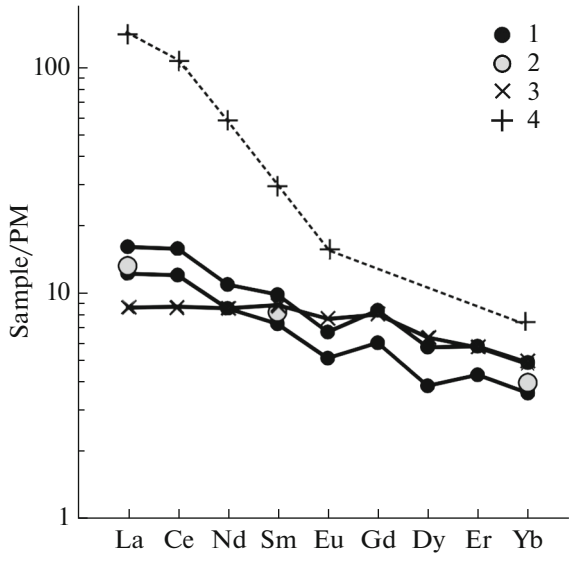

Fig. 4. Primitive mantle-normalized distribution patterns of rare earth elements in inclusions and crustal shale. (1) Melt from a homogenized inclusion in olivine of the basalt, (2) groundmass glass, (3) homogenized inclusion in olivine from the picrite of Disko I., and (4) crustal shale (Pedersen, 1985).

groundmass glass. Similar inclusions and combined melt–fluid inclusions were observed in olivine.

Cryometric investigation. The behavior of fluid bubbles in the groundmass glass during cooling showed that some of them contain complex hydrocarbons, whereas others are dominated by methane. The former were described in detail by Solovova et al. (2002). It was found that cooling to −107°C resulted in instantaneous crystallization of phases on the inclusion walls (Fig. 5a); these phases were rapidly coarsened during heating to −(90–70)°C (Fig. 5b) and melted between −82.6 and −73°C. This temperature was interpreted as the solidus temperature of the complex system. The melting of euhedral crystals of another phase grown by repeated heating and cooling (Fig. 5c) began at −(36.6–32.4)°C. Their complete melting was observed between −31.5 and −26.7°C. It should be noted that sublimation rather than melting could occur in the low-density gas inclusions during heating.

In some inclusions, cooling was accompanied by the crystallization of gas hydrate, which was melted at 7.5–9.0°C (20°C in a single case). Hydrate formation is characteristic of all hydrophobic gases (CO_2, CH_4, C_2H_4, C_2H_6, and other hydrocarbons). These observations indicate the presence of H_2O in the fluid, which is supported by the finding of liquid water rims in some

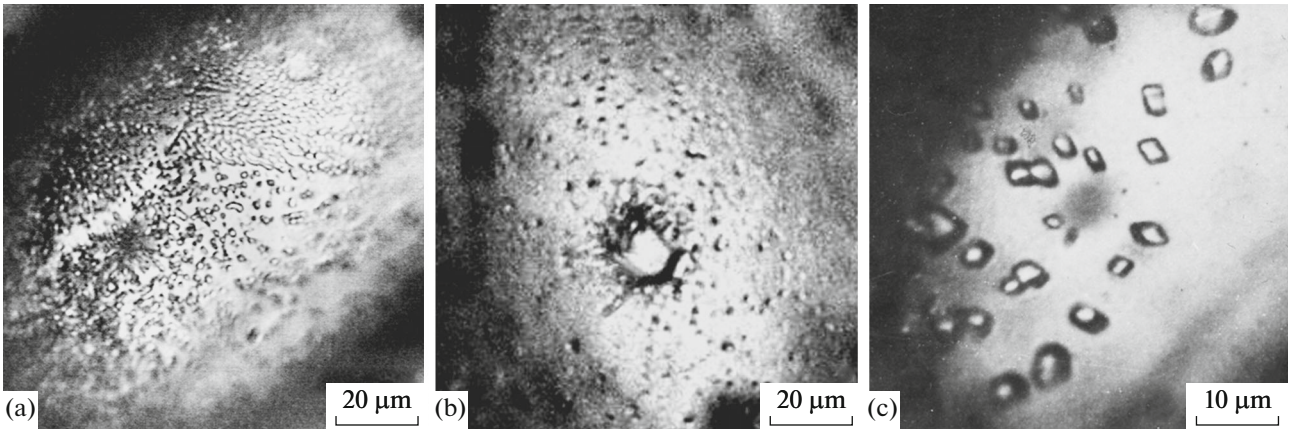

Fig. 5. Behavior of fluid inclusions in groundmass glass during cryometric measurements. (a) Crystallization of phases at –107°C, (b) a monocrystal grown at temperatures between –90 and –70°C, and (c) euhedral crystals of a hydrocarbon phase stable at temperatures from –36.6 to –26.7°C.

vesicles. The size of the gas vesicles and the amount of liquid in them are too low for reliable registration of phase transition during thermometric experiments. The measurement of inclusion filling indicated fluid densities of 0.2–0.3 g/cm^3, which correspond to pressures of 0.15–0.20 GPa during magma crystallization at a temperature of 1200°C (Mel'nik, 1978).

The phase transitions described above were not observed in most fluid inclusions. In such a case, a gas–liquid phase boundary appeared in the inclusions upon cooling to –140°C, which is characteristic of methane. Unfortunately, the temperature of the appearance of the two-phase assemblage could not be measured more precisely.

Raman spectroscopy. Taking into account the unusual behavior and multiphase compositions of fluids during cooling experiments, the inclusions were investigated by Raman spectroscopy. The obtained spectra are shown in Fig. 6. It was found that the optically opaque phase is graphite (Raman peaks at 1361 (D), 1582 (G), 2715, and 3254 cm^{-1}). The very low intensity ratio I(D)/I(G) ~ 0.08 corresponds to a highly ordered graphite modification. The gas phase is a mixture of dominant CH_4 (2917 cm^{-1}) with CO_2 (1284 and 1387 cm^{-1}) and N_2 (2330 cm^{-1}). The Raman spectra of some gas bubbles in the groundmass glass exhibit an H_2 peak. The presence of H_2 in the fluid was expected, because the optical examination of the sample revealed that many gas bubbles are surrounded by lighter colored glass rims (Fig. 1f), which was attributed to iron reduction to FeO owing to hydrogen diffusion trough the bubble walls. The IR spectra of some inclusions contain a minor broad peak at 3334 cm^{-1}, which is indicative of the presence of H_2O.

The density of CO_2 in the fluid bubbles of the groundmass glass was estimated as ~0.2 g/cm^3, which corresponds to a pressure of 50 MPa at a temperature of 770°C (minimum temperature of glass softening in the experiments).

DISCUSSION

In the C–H–O system, the association and proportions of compounds are controlled by the redox regime: CO_2 and H_2O dominate at high oxygen potentials, whereas hydrocarbon fluid (mainly, CH_4) and graphite are formed under reducing conditions (Ryabchikov, 1985). Solovova et al. (2002) showed that melts can be in equilibrium with metallic Fe at a temperature of 1450 K at a log$f$O$_2$ value of –13.95. The calculated composition of C–O–H fluid in equilibrium with metallic Fe, cohenite, and troilite at the estimated oxygen fugacity is shown in Fig. 7. According to these calculations, the fraction of water is no higher than 0.1. At pressures of 20–50 MPa, H_2 is the major component, but methane associating with graphite dominates during olivine crystallization at 0.1 GPa. Methane is the only hydrocarbon that may occur in high-temperature magmas. The Raman spectroscopic investigation of inclusions performed by us supports the results of calculations.

The complex composition of the fluid and coexistence of reduced and oxidized gases: methane, nitrogen, hydrogen, carbon dioxide, and water in association with graphite are probably related to the very rapid cooling (quenching) of the crystallizing magma. Under such conditions, the gas system did not attain equilibrium.

The behavior of inclusions during cryometric measurements provided evidence for hydrocarbon-dominated fluid composition. Naphthalene and its homologues were detected in high-pressure magmatic hydrocarbon inclusions. In our opinion, hydrocarbons other than methane detected in some fluid bub-

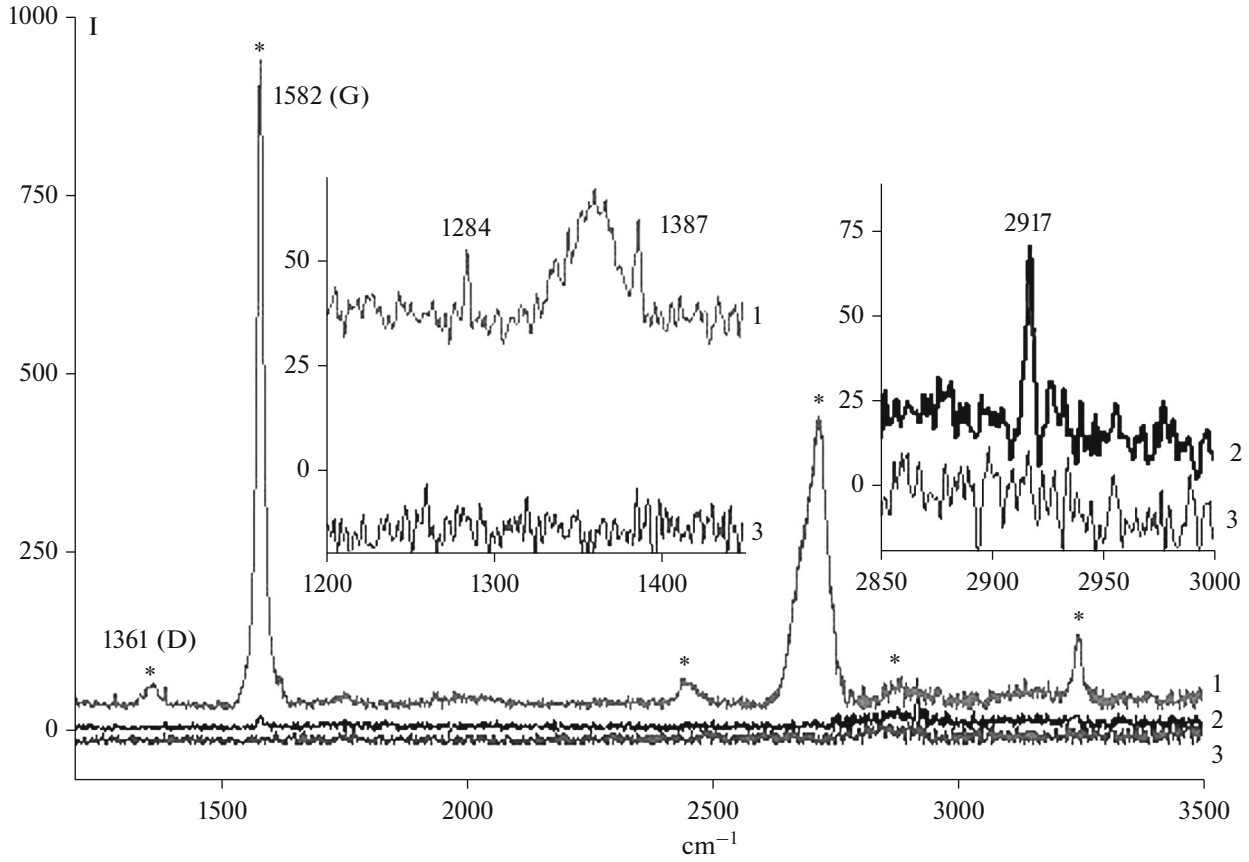

Fig. 6. Raman spectra of fluid phases. (1) Graphite (*) and CO_2 (in inset) peaks in fluid; (2) CH_4 in fluid; and (3) olivine near fluid inclusions. The peaks denoted G and D correspond to the structurally ordered modification of graphite. I is peak intensity, and Raman shift in cm^{-1} is shown along the *x*-axis.

bles in the groundmass glass were formed only during postmagmatic stages at a significant decrease in temperature. Reduced fluids containing hydrocarbons are characteristic of alkaline igneous rocks from Greenland and the Kola Peninsula (Petersilie and Sorensen, 1970; Kogarko et al., 1986; Nivin, 2002). Some authors argued that they were formed during the postmagmatic stages of evolution, but there is also compelling evidence for the presence of primary methane in deep magmas (Ballhaus, 1995). Indeed, the detection of methane in high-temperature inclusions in olivine from the basalts studied by us indicates that reduced gases existed already at the early stages of magma crystallization (cogenetic melt and fluid inclusions and combined varieties were trapped by olivine). However, the abundance of fluid bubbles in the rock suggests a considerable amount of volatile components, which is not typical of deep melts. The question therefore arises as to the source of these fluids.

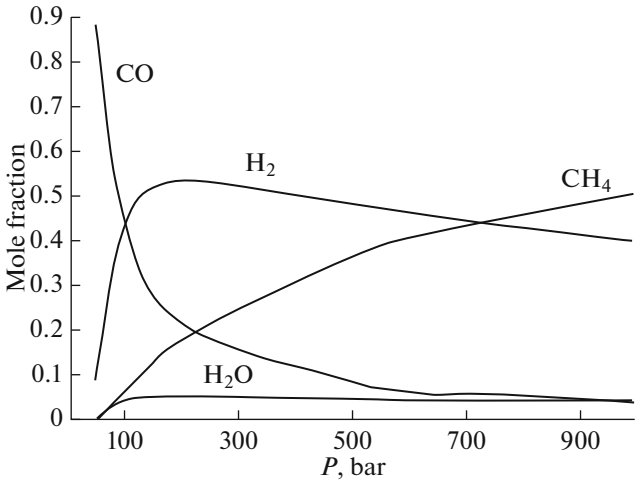

Fig. 7. Composition of fluid in equilibrium with metallic Fe, Fe_3C, and FeS at 1470 K as a function of pressure.

Carbonaceous shale xenoliths containing graphite and Fe–Ni alloy were described by Pedersen (1979) in basaltic dikes with metallic iron from Disko I. Their short-term heating to 1200°C at entrainment into hot magma could result in the formation of a reducing medium. The brevity of their interaction with magma is supported by the behavior of trace elements in melt

inclusions. In particular, minor enrichment of melt was established: LREE/HREE is no higher than 3.4.

Grinenko et al. (1996) estimated the contents and proportions of low-temperature and high-temperature components on the basis of ^{13}C systematics in the mafic volcanic rocks of Disko I. and argued that the basalts contain carbon from different sources, including crustal ones. They concluded that the magma could be enriched at high temperatures in both isotopically heavy carbon of sedimentary carbonates and isotopically light carbonates produced by the partial oxidation of graphite (former organic matter).

Thus, the combined investigation of basalt containing sulfide and metallic alloy allowed us to conclude that the primary magma crystallized under reducing conditions imposed by its short-term interaction (contamination) with carbonaceous shales of crustal origin.

REFERENCES

Albright, D.L. and Kraft, R.W., Structural characteristic of the Fe–FeS eutectic, *Trans. Metall. Soc. AIME,* 1966, vol. 236, pp. 998–1003.

Ballhaus, C., Is the upper mantle metal-saturated?, *Earth Planet. Sci. Lett.,* 1995, vol. 132, pp. 75–86.

Bird, J.M. and Weathers, M.S., Native iron occurrences of Disko Island, Greenland, *J. Geol.,* 1977, vol. 85, pp. 359–371.

Blau, P.J. and Goldstein, J.I., Investigation and simulation of metallic spherules from lunar soil, *Geochim. Cosmochim. Acta,* 1975, vol. 39, pp. 305–324.

Dubessy, J., Poty, B., and Ramboz, C., Advances in C–O–H–N–S fluid geochemistry based on micro-Raman spectrometric analysis of fluid inclusions, *Eur. J. Mineral.,* 1989, vol. 1, pp. 517–534.

Florentin, L., Deloule, E., Faure, F., and Mangin, D., Chemical 3D-imaging of glass inclusions from Allende (CV3) olivine via SIMS: a new insight on chondrule formation conditions, *Geochim. Cosmochim. Acta,* 2018, vol. 230, pp. 83–93.

Frezzotti, M.-L. and Peccerillo, A., Diamond-bearing COHS fluids in the mantle beneath Hawaii, *Earth Planet. Sci. Lett.,* 2007, vol. 262, pp. 273–283.

Grinenko, L.N., Lightfoot, P., and Krouse, R., Unusual isotopic composition and concentrations of carbon in West Greenland mafic volcanic, *Geochem. Int.,* 1996, vol. 34, no. 11, pp. 958–967.

Howarth, G.H., Day, J.M.D., Pernet-Fisher, J.F., et al., Precious metal enrichment at low-redox in terrestrial native Fe-bearing basalts investigated using laser-ablation ICP–MS, *Geochim. Cosmochim. Acta,* 2017, vol. 203, pp. 343–363.

Kogarko, L.N., Kostal'yani, Ch., and Ryabchikov, I.D., Geochemistry of reduced fluid of alkaline magmas, *Geokhimiya,* 1986, no. 12, pp. 1688–1695.

Kullerud, G. and Clark, L.A., *Fe–S System, Carnegie Inst., Yearbook,* 1959, vol. 58.

Kullerud, G., *The Fe–Ni–S system*, *Carnegie Inst. Yearbook,* 1963, vol. 62.

Medenbach, O. and El Goresy, A., Ulvöspinel in native iron-bearing assemblages and the origin of these assemblages in basalts from Ovifak, Greenland, and Bühl, Federal Republic of Germany, *Contrib. Mineral. Petrol.,* 1982, vol. 80, pp. 358–366.

Mel'nik, Yu.P., *Termodinamicheskie svoistva gazov v usloviyakh glubinnogo petrogeneza* (Thermodynamic Properties of Gases under the Conditions of Deep-Seated Petrogenesis) Kiev: Naukova dumka, 1978.

Nivin, V.A., Gas concentrations in minerals with reference to the problem of the genesis of hydrocarbon gases in rocks of the Khibiny and Lovozero complexes, *Geochem. Int.,* 2002, vol. 40, no. 9, pp. 883–898.

Pedersen, A.K., Basaltic glass with high-temperature equilibrated immiscible sulphide bodies with native iron from Disko, central West Greenland, *Contrib. Mineral. Petrol.,* 1979, vol. 69, pp. 397–407.

Pedersen, A.K., *Reaction between picrite magma and continental crust: Early Tertiaty silicic basalts and magnesian andisites from Disko, West Greenland*, *Bull. Grenl. Geol. Unders.,* 1985.

Pedersen, A.K. and Pedersen, S., Sr isotope chemistry of contaminated tertiary volcanic rocks from Disko, central West Greenland, *Bull. Geol. Soc. Denmark,* 1987, vol. 36, pp. 315–336.

Petersilie, I.A. and Sorensen, H., Hydrocarbon gases and bituminous substances in rocks from the Ilimaussaq alkaline intrusion, South Greenland, *Lithos,* 1970, vol. 3, pp. 59–76.

Ryabchikov, I.D., *Mobilization of matter by fluids in the Earth's crust and upper mantle, Kriterii otlichiya metamorfogennykh i magmatogennykh gidrotermal'nykh mestorozhdenii.* (Critteria for the Discrimination between Metamorphogenic and Magmatogenic Hydrothermal Deposits), Novosibirsk: Nauka, 1985, pp. 64–71.

Ryabchikov, I.D., Kogarko, L. N., and Solovova. I.P., Physicochemical conditions of magma formation at the base of the Siberian plume: insight from the investigation of melt inclusions in the meymechites and alkali picrites of the Maimecha–Kotui province, *Petrology,* 2009, vol. 17, no. 3, pp. 287–299.

Sobolev, A.V., Melt inclusions in minerals as a source of principle petrological information, *Petrology,* 1996, vol. 4, no. 3, pp. 209–220.

Solovova, I.P., Ryabchikov, I.D., Girnis, A.V., et al., Reduced magmatic fluids in basalt from the island of Disko, central West Greenland, *Chem. Geol.,* 2002, vol. 183, pp. 365–371.

Solovova, I.P., Kogarko, L.N., and Averin, A.A., Conditions of sulfide formation in the metasomatized mantle beneath East Antarctica, *Petrology,* 2015, vol. 23, no. 6, pp. 519–542.

Translated by A. Girnis